33RD CONGRESS
OF THE INTERNATIONAL COUNCIL
OF THE AERONAUTICAL SCIENCES
STOCKHOLM, SWEDEN, 4-9 SEPTEMBER, 2022

ICAS 2022 SWEDEN

Research on the Effect of the Process first shot peening strengthening then shot peening forming on Fatigue Strength of 7050 High-Strength Aluminum Alloy

Li Guowei[1]，Luo Tianhao[2]，Huang Heyuan[2,3,*]

[1]School of civil aviation, Northwestern Polytechnical University, Xi,an, 710072, China
[2]School of Aeronautics, Northwestern Polytechnical University, Xi,an, 710072, China
[3]Aircraft Strength Research Institute, Aviation Industries of China, Xi'an, 710069, China
*Corresponding author: Huang Heyuan. E-mail: huangheyuan@nwpu.edu.cn.

Abstract

In this paper, the effects of the process first shot peening strengthening then shot peening forming（S+F） on the fatigue strength of 7050 high-strength aluminum alloy were studied by combining experimental testing with numerical simulation. Select the DFR cutoff value as an assessment standard, DFR and residual stress of test pieces with different pit diameters were measured through texts. Furthermore, the residual stress field was fitted and defined by polynomial in MATLAB, and then the small unit stress was set by SIGINI subroutine and its static stress field was simulated by ABAQUS, and then the stress field file was imported into Fe-Safe for fatigue analysis and calculation. The experimental and simulation results show that the model can accurately simulate the fatigue strength of materials. At the same time, the process of strengthening before forming can effectively avoid the stress concentration on the surface of the test parts, which improves the overall fatigue strength. Compared with 1.2mm pit diameter, the fatigue strength of 1.4mm pit diameter test piece is increased by 6.24%.

Keywords: the Process first shot peening strengthening then shot peening forming，Fatigue strength, DFR, Pit diameter

1.Introduction

7050 aluminum alloy has been widely used in the main bearing members of aircraft because of its light weight and high strength[1][2]. However, the long-term alternating load will lead to the fatigue performance of these components, therefore, the aerospace components usually use shot peening strengthening process to enhance the fatigue performance of the components. In recent years, the integration of the aircraft wall plate forming process has become increasingly mature, and the shot peening strengthening process is gradually replaced by the shot peening forming process because it cannot adapt to the trend of integration[3]. Although the introduction of the shot peening forming process can make the aircraft wall plate integrated forming but the fatigue performance of the component has been reduced[4]. In order to solve the fatigue degradation problem caused by the shot peening forming process, researchers are now studying the effect of the new shot peening process on the fatigue performance of specimens. Wang et al[5]. studied the effect of shot peening size on the fatigue performance of specimens with the S+F process and found that a 1.2 mm shot peening increased the DFR benchmark value of specimens by 31%. Marteau and Men et al[6][7]. investigated the effect of ultrasonic amplitude on shot peening strength, saturation time and roughness and found that the strength value and amplitude were negatively correlated and the saturation time and amplitude were positively correlated

The above study shows that although the introduction of other processes after forming improves the fatigue strength of the specimen, it will cause the curvature of the specimen to change and affect the structural forming accuracy[8][9]. Therefore, in this paper, the effect of different forming shot sizes on the fatigue performance of the structure is investigated by using a peening followed by S+F process. Based on the DFR cut-off value as the assessment standard, a finite element model of the DFR cut-off value of the specimen was established based on the numerical method, and the effect law of the S+F process with different forming sizes on the fatigue performance of 7050 aluminum alloy was clarified by combining the test and finite element simulation results with comparative analysis.

2.Text planning

2.1 DFR text

In this section, the DFR cutoff [10]value test was carried out. The test material was 7050 aluminum alloy, and there were 2 groups of specimen,1.2mm pit diameter and 1.4mm pit diameter, 8 specimen in each group. The test schematic is shown in Figure 1. In the test, both ends of the specimen are fixed by the tester chuck, and the tester controls the lower chuck to move down at a rate of 2mm/min to achieve DFR test loading.

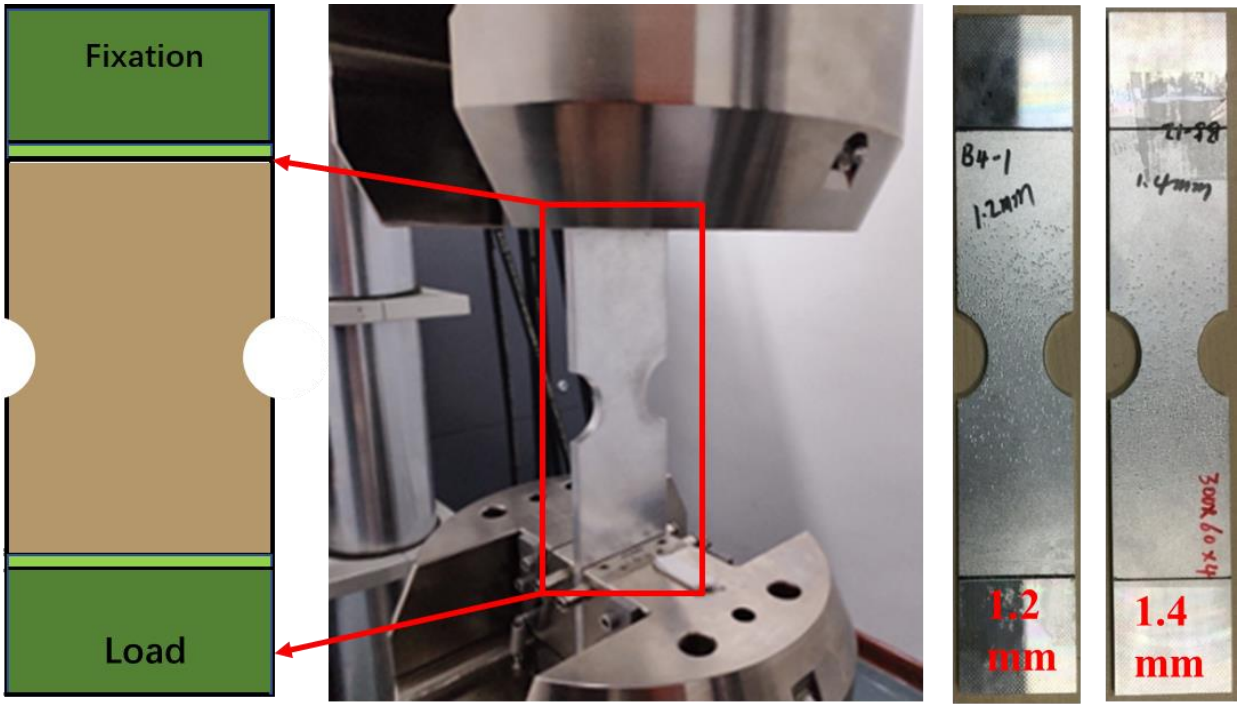

Figure 1 Schematic diagram of the specimen

After the test, single point method and Weibull distribution were used to calculate DFR by introducing relevant parameters[11] (shape parameters, reliability parameters, sample coefficient). Table 1 shows the calculated DFR test values.

Table1 the texts results of DFR

Group	material	diameter	DFR/MPa	ascension
1	7050	1.2mm	188.43	6.24%
2		1.4mm	200.19	

2.2 Residual stress text

In this section, the residual stress measurement test is conducted according to ASTM E915 test standard for the large crater area of shot peening and the area subject to shot peening only. The test

was performed using a μ-360s X-ray diffractometer (Figure 2(a)) with an X-ray tube operating voltage and current of 30KV and 3mA, respectively, and the target material used was a chromium target. The measurement method was the cosα method with a sample distance of 65mm and a measurement range of about 2mm diameter spot. The test position was in the center of the sample, and the residual stresses were tested at the position of surface, 50μm, 100μm, 200μm, 400μm, 600μm and 800μm along the length of the sample. To test the residual stress in the depth direction, brine electrolytic corrosion was used for stripping corrosion with a water ratio of 1:4, and the residual stress was measured after layer-by-layer electrolytic corrosion. It was found that the depth and size of the residual stress in the secondary impact area of the formed projectile increased to different degrees, with the depth of the residual stress layer increasing by about 24.5% and the maximum residual stress level increasing by 16.1%, and the test results are shown in Figure 2(b).

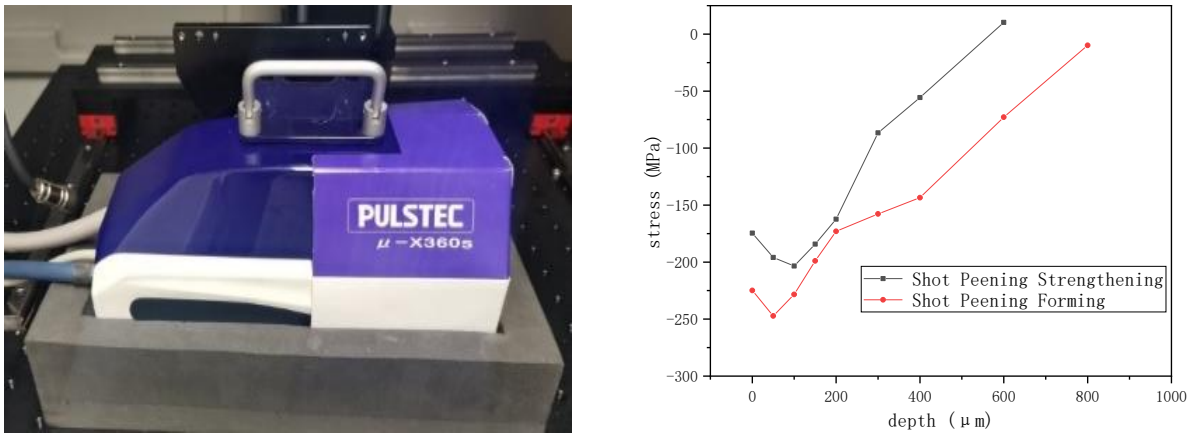

（a） μ-360s portable residual stress meter （b） Residual stress test results

Figure 2 Residual stress test

3.Numerical simulation

3.1 Model building

Firstly, a DFR cut-off test part model is established, and the residual stress field at the shot peening crater and the shot peening residual stress field (defined separately in the SIGINI subroutine) are introduced into the model and then a general analysis step is performed to balance the introduced residual stresses to obtain the final static residual compressive stress field. The stress-strain field file is then imported into Fe- safe to define the material properties, set the fatigue algorithm, and perform fatigue analysis calculations on the model.

Considering that the area affected by the residual compressive stress of a single crater is very small, the difference between the residual stress distribution of the crater simulated in a square area and that simulated in a circular area is very small, so the residual stress is applied to a single crater in a square area of about 1.5 mm. The location of the crater is defined using the normal distribution method, and coordinates obeying the normal distribution are generated by a random algorithm over the entire specimen surface, and the residual compressive stresses in the crater area are given by the test in the cell where these coordinates are located. For the non-pit area, the residual stress distribution of the shot peening layer measured by the test is used.

The size of the model is equal to the DFR cutoff value specimen, the size is 300*60*4, the width of the central section is 30mm, the mesh is divided by hexahedral mesh with neutral axis algorithm, the mesh width is 1.5mm, a total of 198950 C3D8R cells are divided, the whole model cell type is C3D8R cell (eight-node linear hexahedral reduced integral cell), the test piece The meshing of the test part is shown

in Figure 3.

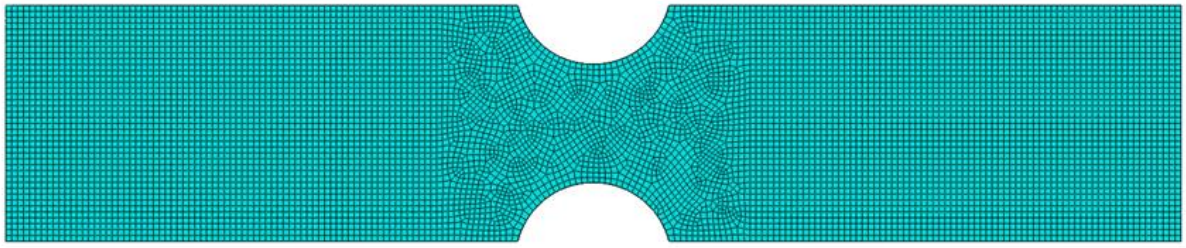

Figure 3 Specimen meshing

3.2Introduction of residual stress

The measured value of residual stress cannot be directly applied to the model surface, and the stress in each cell needs to be set by coordinates through the SIGINI subroutine, but considering the huge number of cells, it is impossible to assign values to each cell individually, so the residual stress field is fitted polynomially in MATLAB, and the residual stress layer on the model surface is defined by means of function definition, In order to get a more accurate residual stress distribution, the surface cells need to be refined along the thickness direction, and the thickness of each layer is set to 0.1 in the range of 0~0.5 and 5.5~6 in the surface layer, and the thickness of each cell is set to 0.5 in the range of 0.5 to 5.5. The shot peening process uses full coverage, so only the thickness aspect of the stress distribution is assigned to the program.

The random coordinates of normal distribution are used for the selection of the shaped crater region, using the transformation principle proposed by Box and Muller. Box-Muller transformation is a method to create random variables obeying normal distribution by random variables obeying uniform distribution. The stress distribution after the introduction of the residual stress field is shown in Figure 4. The local enlargement of the crater is shown in Figure 5.

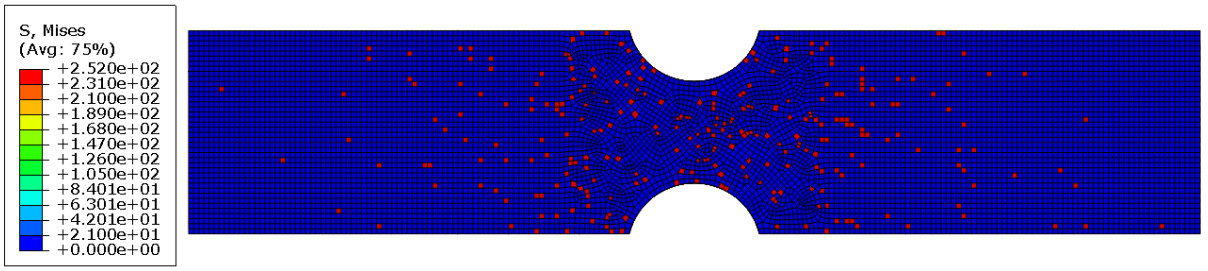

（a） shot peening forming process

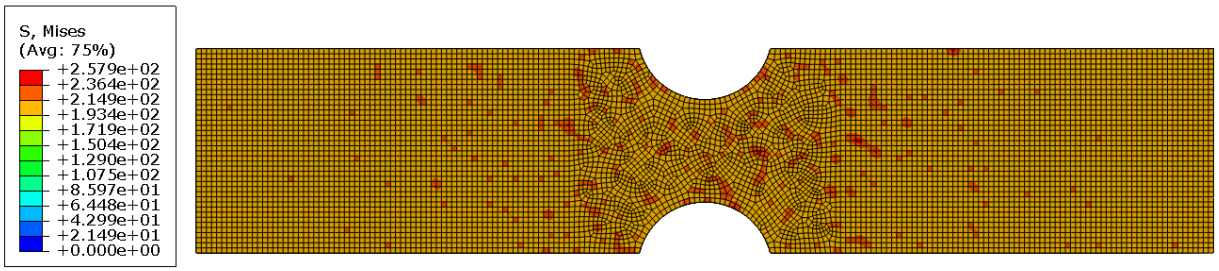

（b） S+F process

Figure 4 Residual stress field distribution

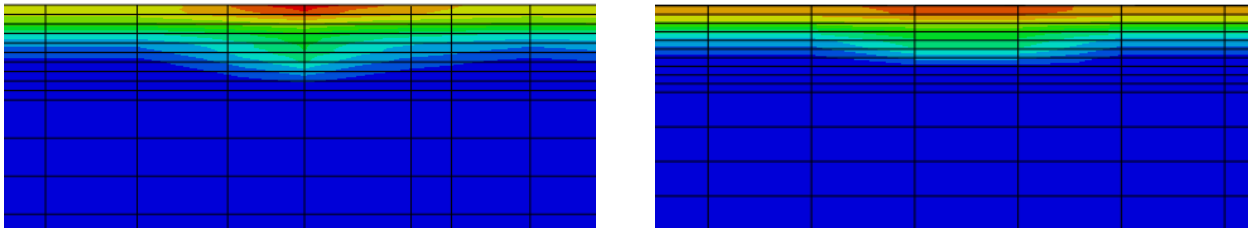

（a）1.4mm pit diameter　　（b）1.2mm pit diameter

Figure 5 partial crater

4. Results and Discussion

4.1 Static analysis

The material properties were defined according to the measured results of the test material parameters. Considering the very small change in modulus before and after the shot peening process, it can be deduced that the difference between 1.2 mm and 1.4 mm processes would be even smaller, so the same material parameters were used for both in this numerical simulation and only the difference in residual compressive stress field was considered. According to the fatigue test boundary conditions, a fixed constraint is applied to the left end of the plate and a constant load is applied to the right end, and the load level is kept the same as that used in the test. 7050 aluminum alloy base value plate with 1.2mm forming process and 1.4mm forming process has the stress cloud shown in Figure 6.

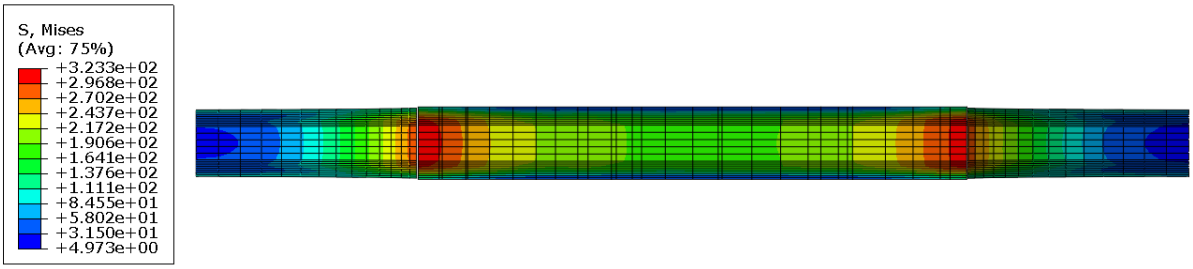

（a）Stress cloud of 1.2mm pit diameter specimen

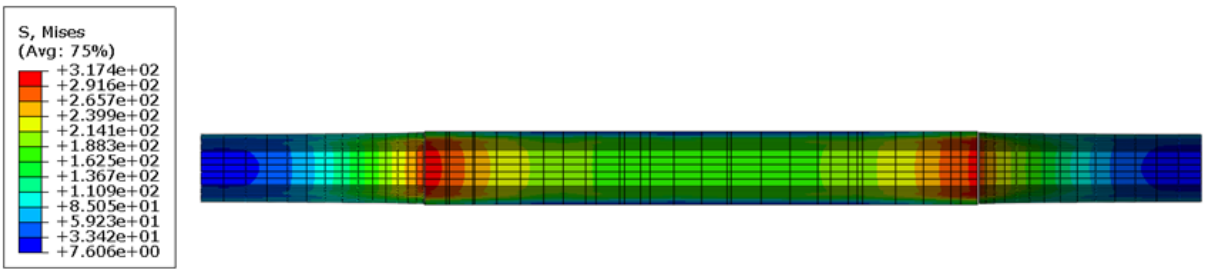

（b）Stress cloud of 1.4mm pit diameter specimen

Figure 6 Stress cloud

The stress cloud above shows that after the introduction of residual compressive stress, the load-induced tensile stress is concentrated on the secondary surface, which will effectively avoid the rapid sprouting of surface cracks due to the surface defects left after the impact of the projectile and the elevated surface roughness. Observing the stress distribution of the cross-section at the notch of the specimen at the cut-off value, the maximum area of stress concentration is located on the meridional

interface at the edge of the notch, and decreases with the increase of the distance from the notch, Figure 7 gives the Mises stress distribution along the longitudinal direction of the central cross-section.

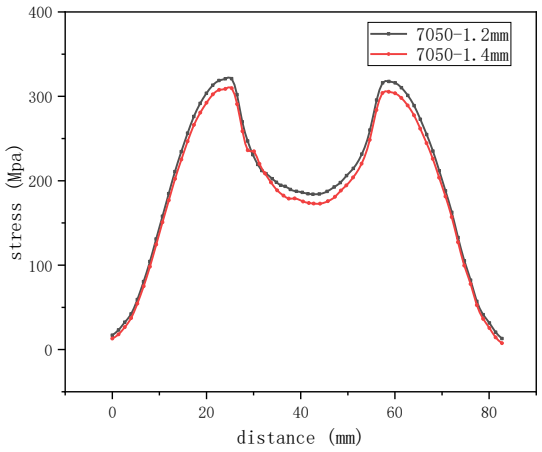

Figure 7 Mises stress distribution

From the figure 7, it can be seen that whether the 1.4mm process or the 1.2mm stress concentration area changes basically do not change, but after using the 1.4mm forming process compared to the 1.2mm process in the dangerous section of the stress concentration is lower, the highest location of the stress concentration in the dangerous arc section decreased by about 5.8%, in both sides of the non-dangerous arc section decreased by about 2.2%, thus it can be seen that the It can be seen that the change to 1.4mm process can play a certain role in reducing the stress level at the critical position of the test piece, and thus improve the overall fatigue performance of the material.

4.2 Fatigue Calculation

By using ABAQUS finite element analysis software, the modeling of the DFR cutoff specimens was completed. Considering the fact that in this study, the S+F process is used, a large number of forming craters will be generated on the surface of the sheet metal, and the residual stress field distribution in the crater area is significantly different from the residual stress field in the area not affected by the forming craters. Therefore, the residual stress fields of shot peening strengthening and shot peening forming are considered separately in the whole analysis process. By refining the model surface, the stress fields measured in the residual stress test are imported into the model through the SIGINI subroutine, and finally the calculated stress-strain fields are imported into Fe-safe for fatigue analysis calculation, and the whole analysis process is shown in Figure 8.

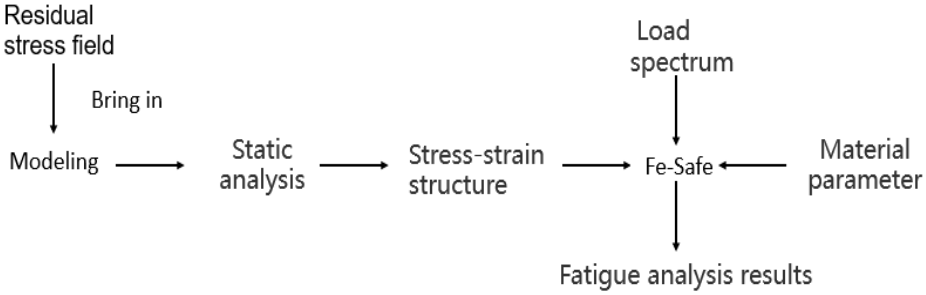

Figure 8 Fatigue life analysis process

The stress field obtained from the simulation was imported into Fe-Safe for fatigue calculation. Figure 9 shows the fatigue simulation results, and Table 2 shows the comparison between the experimental and simulated values.

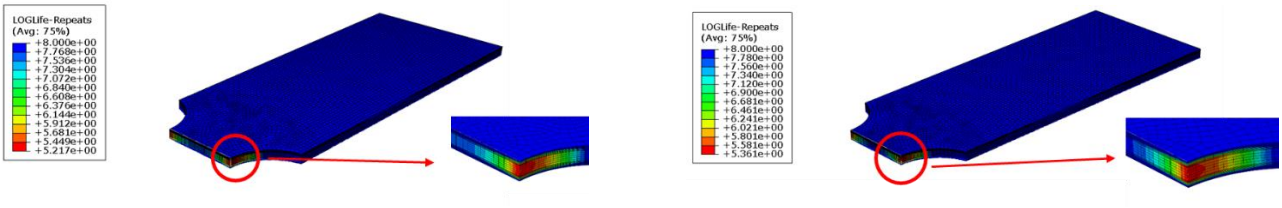

(a) 12mm pit diameter process (b) 1.4mm pit diameter process

Figure 9 Fatigue simulation results

Table 2 Comparison of DFR values

Group	Load/MPa	Fatigue life	DFR simulation value /MPa	DFR test results /MPa	Error
1.2mm	206	164816	171.8	188.4	9.6%
1.4mm	206	229614	184.6	200.2	8.4%

During modeling and testing, it was found that fatigue cracks were firstly generated in the middle section of the arc; the simulation also showed that the stresses were concentrated on the secondary surface, which effectively avoided the rapid sprouting of surface cracks due to surface defects left after projectile impact and surface roughness enhancement; the fatigue strength of the 1.4mm crater diameter was improved by about 6.24% compared with that of the 1.2mm crater diameter test piece, and the former resulted in the overall material fatigue performance was improved.

5. Conclusion

In this paper, the effect of shot peening and forming and strengthening process on the fatigue strength of 7050 aluminum alloy was investigated based on the experimental method, and then a random shot peening model was established by ABAQUS, and the fatigue strength of the numerical model was calculated by using FE-SAFE. It was found that compared with the crater size of 1.2mm used for the forming process, the 1.4mm crater size can lead to a certain improvement in fatigue strength, which is about 6.24% for the test piece with a low stress concentration factor cutoff value.

6. Acknowledgments

This work was jointly supported by the General Project of Chongqing Natural Science Foundation (No. cstc2020jcyj-msxmX0784) and China Postdoctoral Science Foundation (2021M693007).

7. Contact Author Email Address

Email: 1278282948@qq.com

8. Copyright Statement

Reference

[1] Fu X L, Zhou B, Meng Y, Pan Y Z, Study on the constitutive model of anisotropic aluminum alloy in high speed cutting, Mach Sci Technol, Vol. 24, No. 6, pp. 906-923, 2020.

[2] Azam S, Nayebi N, Hojjatollah R, Application of anisotropic continuum damage mechanics in ratcheting characterization, Mech Adv Mater Struc, Vol. 29, No. 1, pp. 70-77, 2020.

[3] Shi S G, Wang M T, Bai X P, Chen F L, Deformation law of 7B50 aluminum alloy in shot peening for large size projectiles, Forging & Stamping Technolog Vol. 46, No. 3, pp. 96-100, 2021.

[4] Wang M T, Zeng Y S, Huang X, Research on Surface Quality of 2024-T351 Aluminum Alloy by Peen Forming With Large Ball, Aeronautical Manufacturing Technology, Vol. 5, No. 23, pp. 92-94, 2012.

[5] Wang H S, Research and Numerical Simulation of Fatigue Performance of 2024 Alumiuum Alloy Shot Peening Forming Panel, Engineering Technology, Vol. 2022, No. 1, pp. 2021.

[6] Marteau J, Bigerelle M, Mazeran P E, Bouvier S, Relation between roughness and processing conditions of AISI 316L stainless steel treated by ultrasonic shot peening, Tribol Int, Vol. 82, No. pp. 319-329, 2015.

[7] Yang H, Xu G, Zhang W, Li B B, Liang S R, Li F, Application of Ultrasonic Shot Peening Technology in Deformation Correction of Large Parts, Engineering Technology, Vol. 2020, No. 9, pp. 54-56, 2020.

[8] Wang C Y, Li W G, Jiang J J, Chao X, Zeng W K, Yang J, Mechanical behavior study of asymmetric deformation in double-sided symmetrical sequential shot peening process, Int J Adv Manuf Tech, Vol. 114, No. 3-4, pp. 1189-1204, 2021.

[9] Zhong L Q, Liang Y L, Hu H, Study on Plastic Deformation Characteristics of Shot Peening of Ni-Based Superalloy GH4079, International Conference on Materials Sciences and Nanomaterials, Vol. 230,No. pp. 14-16, 2017.

[10] Benedetti M, Fontanari V, Santus C, et al. Notch fatigue behaviour of shot peened high-strength aluminium alloys: Experiments and predictions using a critical distance method[J]. International Journal of Fatigue, 32(10):1600-1611, 2010.

[11] Chieragatti M, Modelling the influence of machined surface roughness on the fatigue life of aluminium alloy[J]. International Journal of Fatigue, 2008.